Journal of Molecular Catalysis A: Chemical 345 (2011) 81–89

Contents lists available at ScienceDirect

Journal of Molecular Catalysis A: Chemical

journal homepage: www.elsevier.com/locate/molcata

Pt nanoparticles entrapped in ordered mesoporous carbon for enantioselective hydrogenation

Bo Li, Xiaohong Li*, Hongna Wang, Peng Wu

Shanghai Key Laboratory of Green Chemistry and Chemical Processes, Department of Chemistry, East China Normal University, 3663 North Zhongshan Road, Shanghai 200062, China

ARTICLE INFO

Article history:
Received 27 January 2011
Received in revised form 19 April 2011
Accepted 26 May 2011
Available online 2 June 2011

Keywords:
Asymmetric hydrogenation
Pt nanoparticles
Ordered mesoporous carbon
Ethyl pyruvate
Ethyl 2-oxo-4-phenylbutyrate

ABSTRACT

Pt nanoparticles entrapped in CMK-3 ordered mesoporous carbon materials, prepared by a facile impregnation method, were found to be efficient for the enantioselective hydrogenation of α-ketoesters by modification with cinchona alkaloids. The initial activity of higher than 23,000 h^{-1} TOF and 82% ee were obtained for the chiral hydrogenation of ethyl pyruvate with cinchonidine (CD)-modified Pt/CMK-3 catalyst. With regard to the chiral hydrogenation of ethyl 2-oxo-4-phenylbutyrate, the CD-modified Pt/CMK-3 catalyst afforded the highest TOF of 5615 h^{-1} and 64% ee. For comparison, commercially available Pt/C and Pt/Al_2O_3 catalysts were investigated as well. The Pt/CMK-3 catalysts were more efficient than the commercial Pt/C catalyst. Of particular note is that the Pt/CMK-3 catalyst exhibited good stability; only below 0.005% Pt atoms were leached into solution after the chiral hydrogenation of ethyl pyruvate in acetic acid, while the Pt leaching amount for the commercial Pt/Al_2O_3 and Pt/C catalysts was 0.15% and 0.25%, respectively. In addition, the Pt/CMK-3 catalyst could also be reused for more than 5 times without distinct loss of activity and enantioselectivity, while the reusability for the commercial Pt/C and Pt/Al_2O_3 catalysts was poor. Based on IR and Raman spectroscopic characterization, it is suggested that both the physical structure features, including high specific surface area, adequate pore volume, ordered mesopores and small Pt particle size with high dispersion, and the chemical nature of catalyst surface with high electron density would improve the performance of Pt/CMK-3 catalysts.

1. Introduction

Enantioselective hydrogenation of α-functionalized ketones to alcohols is an important chemical process owing to great application of chiral alcohols in synthesis of chiral drugs, pesticides, food additives and perfumes, etc. [1–3]. The catalytic enantioselective hydrogenation of α-ketoesters on the supported Pt catalysts after chirally modified with cinchona alkaloids has been regarded as one of the landmarks of heterogeneous asymmetric catalysis [4–8].

Since the heterogeneous enantioselective hydrogenation was firstly reported by Orito and co-workers in 1978 [9–11], many kinds of materials have been adopted to support Pt nanoparticles. In the beginning, inorganic carriers like Al_2O_3, SiO_2, TiO_2, etc. were considered to be suitable supports for Pt nanoparticles, but these materials supported Pt catalysts showed only mediocre performance in the asymmetric hydrogenation of pyruvate esters [12–17], except that CD-modified 5.0 wt.% Pt/Al_2O_3 catalysts induced good to excellent enantioselectivity [12,13]. With the rapid development of molecular sieves and periodic mesoporous materials, MCM-41 [18], HNaY [19] and FDU-14 mesopolymer [20] were adopted as supports for Pt nanoparticles in the heterogeneous asymmetric catalysis, furnishing medium to good enantioselectivities in the chiral hydrogenation of α-functionalized ketones.

Clearly, to the best of our knowledge, alumina supported Pt catalyst seems to be one of the best catalyst for the asymmetric hydrogenation of α-functionalized ketones until now. Nevertheless, the intrinsic drawback of Al_2O_3 with inferior stability in acetic acid limits the reusability of Pt/Al_2O_3 catalysts due to peptization of alumina under the acidic conditions [21]; whereas acetic acid is one of the best solvents for the heterogeneous enantioselective hydrogenation of α-functionalized ketones with cinchona alkaloids modified Pt catalysts.

Carbon materials are one kind of the most rapidly developing advanced materials due to potential applications in heterogeneous catalysis and electrocatalysis. The relevant application of carbon material as support for Pt nanoparticles to the heterogeneous enantioselective catalysis can be traced back to the original work of Ortio and co-workers about the asymmetric hydrogenation of α-ketoesters [10,22], although the results did not arouse concern at that time. More than 20 years later, Fraga et al. [23] investigated in detail the surface chemistry of activated carbon on enantioselective hydrogenation of methyl pyruvate over CD-modified Pt/C catalysts. Under the optimal conditions, up to 35% ee value of (*R*)-(+)-methyl

* Corresponding author. Tel.: +86 21 6223 8590; fax: +86 21 6223 8590.
E-mail address: xhli@chem.ecnu.edu.cn (X. Li).

1381-1169/$ – see front matter © 2011 Elsevier B.V. All rights reserved.
doi:10.1016/j.molcata.2011.05.023

lactate was achieved. Meanwhile, Perosa et al. [24] studied the enantioselective hydrogenation of acetophenone on commercially available Pt/C catalysts after chirally modified with cinchona alkaloids in a biphasic water–isooctane system. For comparison, the chiral hydrogenation of ethyl pyruvate was also carried out under the same conditions. As a result, up to 20% ee was obtained for the chiral hydrogenation of acetophenone; while only 14% ee was acquired for the asymmetric hydrogenation of ethyl pyruvate. However, as well known, the ee value for the chiral hydrogenation of ethyl pyruvate was much higher than that of acetophenone with Pt/Al_2O_3 catalysts in a single phase system [25].

Recently, Xing et al. [26] adopted single-walled carbon nanotubes (SWNTs) to support Pt nanoparticles with different loadings for the heterogeneous asymmetric hydrogenation of ethyl pyruvate. After optimization of reaction parameters, 50% ee of (*R*)-(+)-ethyl lactate was induced with CD-modified 20 wt.% Pt/SWNTs catalyst. Very recently, TiO_2 coated multi-walled carbon nanotubes-supported Pd catalysts have been applied in the enantioselective hydrogenation of a series of α-unsaturated carboxylic acids using CD as chiral modifier, furnishing up to 52% ee for the chiral hydrogenation of (*E*)-α-phenylcinnaic acid [27]. In addition, a highly mesoporous carbon xerogel has also been attempted to support Pd catalyst for enantioselective hydrogenation of isophorone and of 2-benzylidene-1-benzosuberone [28,29]. Although inferior ee values were induced for both substrates, the highly mesoporous carbon xerogel supported Pd catalysts were a little more enantioselective than the more dispersed commercial Pd/C catalyst [30,31].

Ordered mesoporous carbons (OMCs) have attracted much more attention since their discovery, due to periodic mesopores, uniform pore size, high surface areas, adequate pore volume and high thermal, chemical and mechanical stabilities [32–34]. These features make OMCs to be prospective candidates as adsorbents [35], catalyst support and catalyst [36,37], electrode materials [38], and templates for synthesis of nanostructured inorganic materials and mesoporous polymer carbon composites [39,40]. CMK-3 carbons are one kind of the widely studied OMCs, which can be synthesized by a classic two-step nano-casting method, using mesoporous silica SBA-15 as template, sucrose as carbon source, sulphuric acid as carbonization catalyst and carbonized at 1173 K [41]. They have been proved stable even under acidic conditions and also exhibit unique hydrophobic affinity towards organic reactants and solvents [42].

Herein we report the application of CMK-3 as a support to stabilize Pt nanoparticles for the enantioselective hydrogenation of α-ketoesters after chirally modified with CD (Scheme 1). For comparison, the commercially available Pt/C and Pt/Al_2O_3 catalysts were also applied. To the best of our knowledge, this is the first report on the use of CMK-3 OMCs for the preparation of Pt catalysts in the heterogeneous enantioselective catalysis.

2. Experimental

2.1. Materials

Hydrogen hexachloroplatinate (IV) hexahydrate ($H_2PtCl_6{\cdot}6H_2O$), sodium formate and other chemicals were of analytical grade. Pluronic 123 ($EO_{20}PO_{70}EO_{20}$, MW = 5800) was purchased from Sigma–Aldrich. Ethyl pyruvate (98%), ethyl 2-oxo-4-phenylbutyrate (EOPB) (91%) and CD (99%) were purchased from Alfa Aesar (A Johnson Matthey Company) and used as received. The commercial Pt/C (5 wt.%) and Pt/alumina (5 wt.%) catalysts were also purchased from Alfa Aesar. The other commercial Pt/C (5 wt.%) catalyst was purchased from Sigma–Aldrich for comparison. For convenience, the Pt/C catalysts purchased from **A**lfa **A**esar and from **S**igma–**A**ldrich were designated hereinafter as Pt/C-AA and Pt/C-SA, respectively.

2.2. Catalyst preparation

The CMK-3 OMCs were synthesized using mesoporous silica SBA-15 as the hard template, sucrose as the carbon source and sulfuric acid as the carbonization catalyst [41]. The 5.0 wt.% Pt/CMK-3 catalysts were prepared mainly according to Ref. [20]: CMK-3 was impregnated with a solution containing H_2PtCl_6 and stirred for 4–6 h. Then the mixture was evaporated to remove the excess solvent, followed by a drying at 353 K overnight. Subsequently, one portion of catalyst precursor was directly reduced in an aqueous solution of sodium formate, while the other portion was calcined under vacuum at 423 K or at 523 K for 2 h before reduction using the same method. Then the mixture was washed by plenty of water to remove chlorine ions and dried at 353 K overnight. According to the preparation procedures, the obtained Pt/CMK-3 catalysts are denoted as Pt/CMK-3-W/E-T, where W/E represents different diffusion medium of H_2PtCl_6, for example, W represents water and

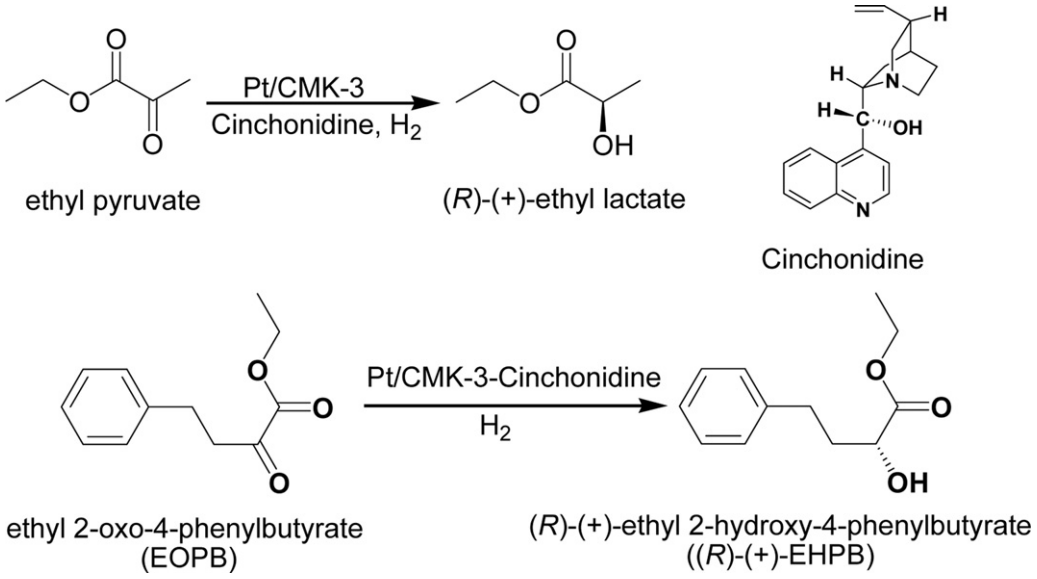

Scheme 1. Enantioselective hydrogenation of ethyl pyruvate and EOPB on CD-modified Pt/CMK-3 catalysts.

E represents ethanol; *T* represents the calcination temperature in Kelvin for the catalyst precursor before reduction. The description without "*T*" stands for the Pt/CMK-3 catalysts without calcination before reduction.

2.3. Characterization

The X-ray diffraction (XRD) patterns of samples were collected on a Bruker D8 Advance instrument using Cu-Kα radiation. The nitrogen adsorption–desorption isotherms were measured at 77 K on a Quantachrome Autosorb-3B system, after the samples were evacuated for 10 h at 373 K. The BET specific surface area was calculated using adsorption data in the relative pressure range from 0.05 to 0.35. The pore size distribution curves were calculated from the analysis of the adsorption branch of the isotherm using the BJH algorithm. The Raman spectrum of CMK-3 carbon was taken on a Renishaw inVia Raman Spectroscopy excited using a 632.8 nm laser. The TEM images were taken on a Jeol JEM-2100 electromicroscopy with an acceleration voltage of 200 kV.

CO chemisorption of samples was measured at 308 K on a Quantachrome CHEMBET-3000 pulse chemisorption analyzer after the samples were pretreated in a 5 vol.% H_2/95 vol.% Ar flow at 673 K for 2 h. The degree of dispersion and the mean particle size (cubic model) were estimated from the measured CO uptake, assuming a cross-sectional area for a surface platinum atom of 8.0×10^{-20} m^2 and a stoichiometric factor of one, using nominal platinum concentrations. The leached amount of Pt atoms into solution after reaction was detected with a Thermo Elemental IRIS Intrepid II XSP inductively coupled plasma-atomic emission spectroscopy (ICP-AES). The surface electronic state of platinum particles was examined by Diffuse Reflectance Infrared Fourier-Transform Spectroscopy (DRIFTS) using CO as probe molecules. The analysis was carried out with a Nicolet NEXUS 670 spectrometer. The catalyst sample was pretreated in a 5 vol.% H_2/95 vol.% Ar stream at 673 K for 2 h, and then was purged with He for 30 min. When the sample was cooled down to 308 K, CO was introduced into the IR cell until the adsorption was saturated. Then the sample was flushed with a He flow before the spectrum was recorded.

2.4. Catalytic tests

For the enantioselective hydrogenation, unless otherwise mentioned, Pt/CMK-3, Pt/C or Pt/Al_2O_3 catalyst (0.026 mmol Pt) was pretreated in a hydrogen flow (40 mL/min) at 673 K for 2 h before use. The catalyst was then mixed with CD (0.034 mmol), ethyl pyruvate (21.07 mmol) or EOPB (5.29 mmol), solvent (20 mL) and transferred to a 100 mL autoclave with magnetic stirring (1200 rpm). The hydrogenation reaction began at room temperature after hydrogen (4.0 MPa) was introduced into the autoclave. The reaction was stopped after a proper time and the products were analyzed by GC-FID (GC 2014, Shimadzu) equipped with a capillary chiral column (HP19091G-B213, 30 m × 0.32 mm × 0.25 μm, Agilent). The optical yield was expressed as ee value: ee (%) = ([*R*] − [*S*])/([*R*] + [*S*]) × 100.

3. Results and discussion

3.1. Catalyst preparation and characterization

The procedures for preparing CMK-3 supported Pt catalysts are graphically illustrated in Fig. 1, which consists of the preparation of CMK-3 replica from SBA-15 and the impregnation of CMK-3 with H_2PtCl_6 dissolved in different media, followed by reduction with sodium formate. Fig. 2 shows the low-angle X-ray diffraction (XRD) patterns of SBA-15 template, CMK-3 replica and the resultant Pt/CMK-3 catalysts. Similar to SBA-15, CMK-3 exhibited an intense diffraction peak together with two weak peaks indexed as (1 0 0), (1 1 0) and (2 0 0) planes of hexagonal struc-

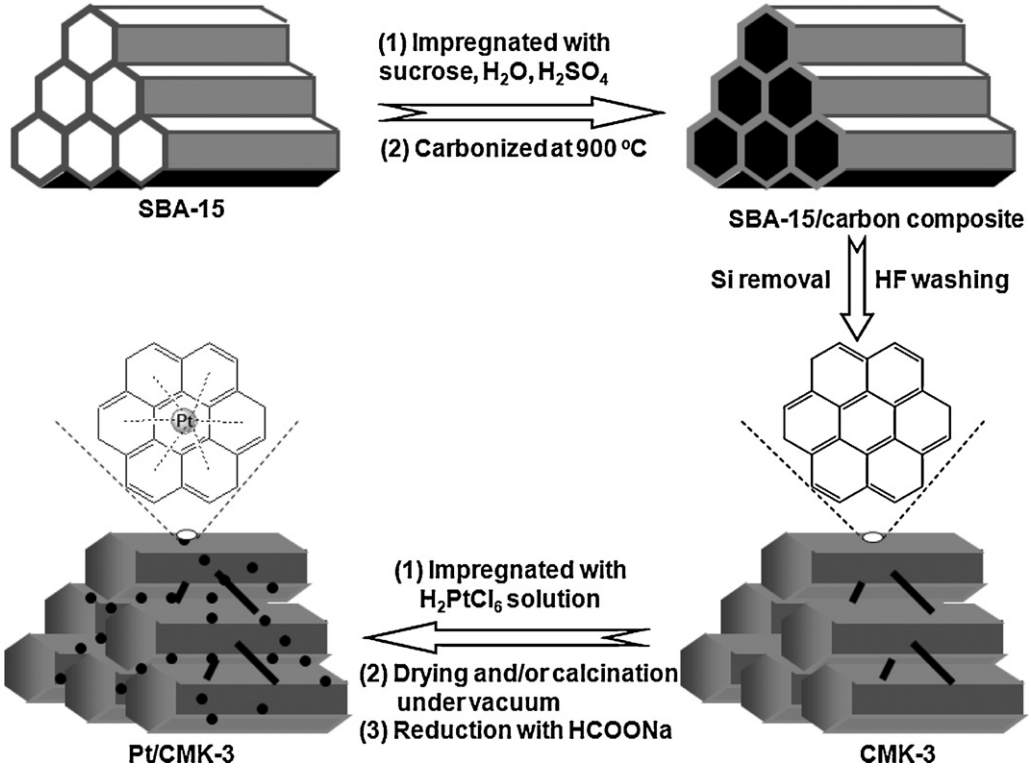

Fig. 1. Schematic illustration for preparation of Pt/CMK-3 catalysts.

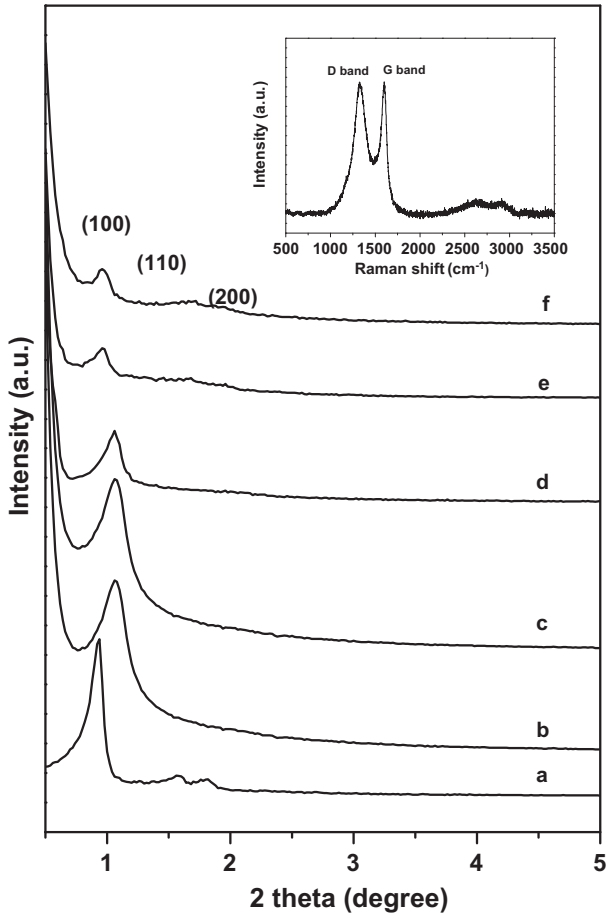

Fig. 2. Low-angle XRD patterns of (a) SBA-15; (b) CMK-3; (c) Pt/CMK-3-W; (d) Pt/CMK-3-E; (e) Pt/CMK-3-W-423; (f) Pt/CMK-3-W-523 and Raman spectrum (inset) of CMK-3 recorded with a laser wavelength of 632.8 nm.

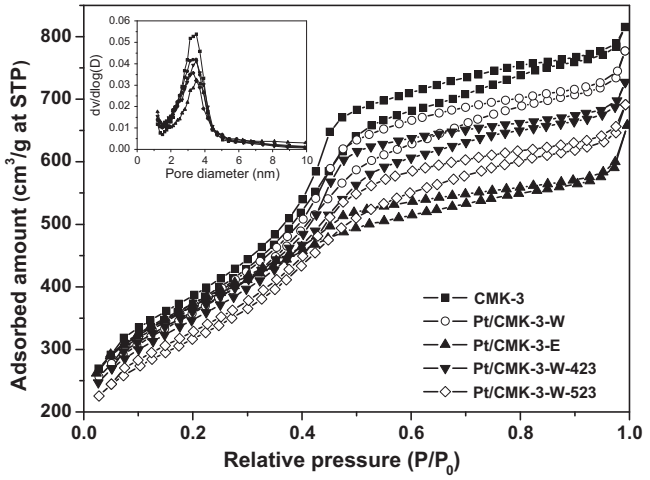

Fig. 3. N_2 adsorption–desorption isotherms and pore size distribution (inset) of CMK-3 and related catalysts.

ture (p6mm). All the Pt/CMK-3 catalysts also displayed the distinct (1 0 0) diffraction, similar to the support CMK-3. This demonstrates that even if the CMK-3 support was impregnated with Pt precursor solution for several hours and in some cases the catalyst precursors were calcined at a high temperature, the meso-structure of CMK-3 was still retained. As for the decreased intensity of (1 0 0) diffraction peak after Pt nanoparticles loading, it can be explained in terms of the reduced contrast between mesopores and pore walls.

The well-ordered mesoporous structure of CMK-3 support could be further confirmed by the N_2 sorption isotherms of Pt/CMK-3 catalysts (Fig. 3). All the Pt/CMK-3 catalysts displayed the typical hysteresis loop in the relative pressure range from 0.45 to 0.8 and also showed narrow BJH pore size distribution centered at 3.5 nm. As listed in Table 1, the specific surface area of CMK-3 was 1325 $m^2\ g^{-1}$, while the specific surface area for Pt/CMK-3 catalysts ranged from 1130 to 1290 $m^2\ g^{-1}$. The Pt/CMK-3 catalysts also had adequate pore volume higher than 1.0 $cm^3\ g^{-1}$. These physical features of Pt/CMK-3 catalysts would certainly be helpful to mass transport.

To obtain further information on the CMK-3 structure, Raman spectroscopy was carried out. The inset of Fig. 2 shows a representative spectrum recorded at a laser excitation wavelength of 632.8 nm in the 500–3500 cm^{-1}. As typically found for sp2 bonded carbons, the spectrum was dominated by the G and D bands, located in this case at 1594 and 1335 cm^{-1}, respectively. The position of the G band, together with the relatively strong intensity of the D band, indicates that CMK-3 carbons mainly consist of disordered graphene with a very small size. The broad and weak features centered at 2627 and 2907 cm^{-1} also suggest existence of small amount of amorphous carbon besides the disordered graphene [43].

The Pt particle size was firstly characterized using the wide-angle XRD (Fig. 4). Except for Pt/CMK-3-W-523 catalyst, the Pt/CMK-3 catalysts did not show the typical diffractions assigned to Pt crystalline indexed as Pt(1 1 1), Pt(2 0 0) and Pt(2 2 0) planes, indicating that the Pt particles were uniformly dispersed on the CMK-3 support and did not aggregate to form large crystalline for Pt/CMK-3 catalysts which were not calcined at above than 423 K. The calcination at 523 K caused strong aggregation of Pt nanoparticles. The morphology of some Pt/CMK-3 catalysts was also characterized using TEM. As can be revealed in the TEM images (Fig. 5), the Pt/CMK-3-W and Pt/CMK-3-E catalysts retained the typical p6mm meso-structure and the Pt nanoparticles were uniformly dispersed inside the CMK-3 mesopores.

The Pt particle size and dispersion were also calculated according to the measured CO chemisorption (also listed in Table 1). In

Table 1
Relevant parameters of CMK-3 and Pt/CMK-3, Pt/C-AA and Pt/Al_2O_3 catalysts.

Sample	S_{BET} ($m^2\ g^{-1}$)	D_{Pore} (nm)	V_{Pore} ($cm^3\ g^{-1}$)	Pt size[a] (nm)	Pt dispersion[a] (%)
CMK-3	1325	3.5	1.26	–	–
Pt/CMK-3-W	1290	3.5	1.18	2.6	43.7
Pt/CMK-3-E	1265	3.5	1.02	2.2	52.5
Pt/CMK-3-W-423	1230	3.5	1.13	2.8	41.2
Pt/CMK-3-W-523	1130	3.3	1.07	10.7	10.6
Pt/C-AA	892	3.8	1.07	10.3	11.0
Pt/Al_2O_3	147	18.4	0.9	3.5	32.8

[a] Pt particle size and dispersion was determined by CO chemisorption.

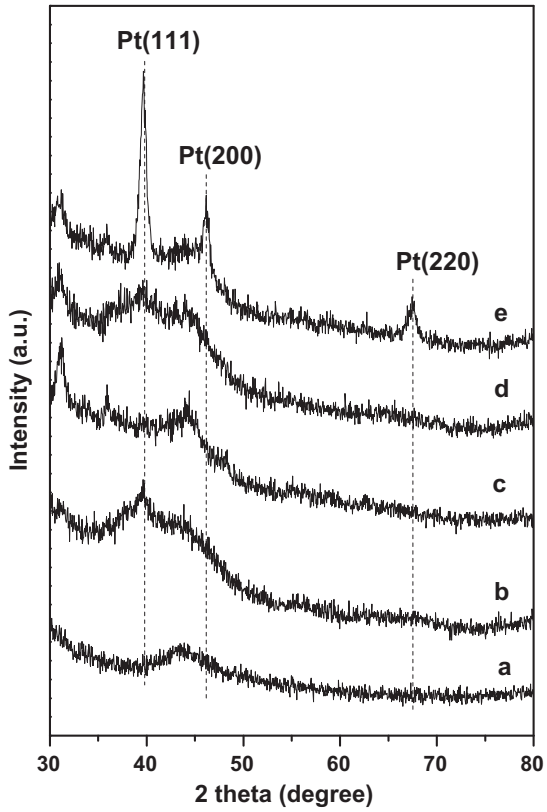

Fig. 4. Wide-angle XRD patterns of (a) CMK-3; (b) Pt/CMK-3-W; (c) Pt/CMK-3-E; (d) Pt/CMK-3-W-423; (e) Pt/CMK-3-W-523.

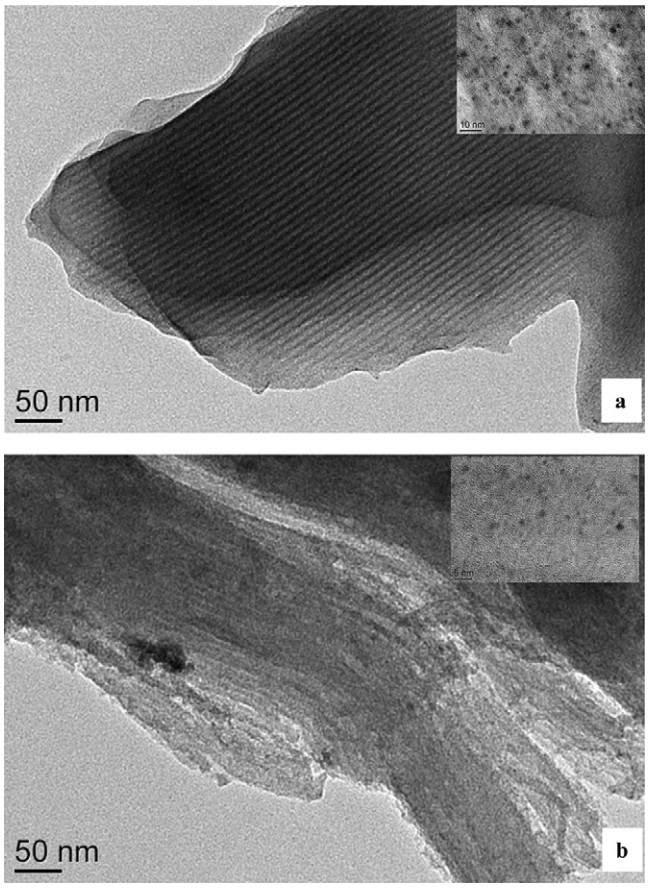

Fig. 5. TEM images of (a) Pt/CMK-3-W and (b) Pt/CMK-3-E. The inset bars in (a) and (b) are 10 nm and 5 nm, respectively.

agreement with the results from the wide-angle XRD and TEM analysis, the average Pt particle size for Pt/CMK-3-W catalyst was around 2.6 nm with 43.7% dispersion, while the average Pt particle size for Pt/CMK-3-E catalyst was around 2.2 nm with 52.5% dispersion. With calcination before reduction, the Pt particle size was increased and as a result; the Pt particle size for Pt/CMK-3-W-423 and Pt/CMK-3-W-523 catalysts were 2.8 and 10.7 nm, respectively.

The relevant physico-chemical parameters for the commercial Pt/C-AA and Pt/Al_2O_3 catalysts are also shown in Table 1. The 5 wt.% Pt/C-AA catalyst also had relatively large surface area and pore volume, but the average Pt particle size was a little bigger (10.3 nm) with lower dispersion (11.0%). For the commercial Pt/Al_2O_3 catalyst, the mean Pt particle size was comparable with that of Pt/CMK-3 catalyst series, although the specific surface area was only 147 $m^2\,g^{-1}$.

3.2. Effect of chiral modifier amount on Pt/CMK-3 catalyst performance

To make sure optimum amount of chiral modifier, we firstly investigated the influence of CD amount on the catalytic performance in the asymmetric hydrogenation of ethyl pyruvate with Pt/CMK-3-W catalyst. Fig. 6 shows the profiles of conversion and ee value *vs* CD amount within 5 min. No addition of CD into the reaction system, only 4.3% of ethyl pyruvate was converted to ethyl lactate without enantioselectivity. When 0.0068 mmol CD was added, 25.3% ethyl pyruvate conversion and 64.5% ee of (*R*)-(+)-ethyl lactate were achieved, suggesting that the Pt/CMK-3-catalyzed asymmetric hydrogenation of ethyl pyruvate was a "ligand-accelerated" reaction.

With increase of CD amount to 0.017 mmol, the conversion of ethyl pyruvate was further improved and the ee value was slightly increased as well. When the CD amount was further increased to 0.034 mmol, both the highest conversion of 81.0% and the highest ee value of 82.2% were obtained. Too high CD concentration (0.051 mmol) caused the conversion and ee value decrease strongly. Consequently, the CD amount of 0.034 mmol was added in the following tests and thus the substrate to CD molar ratio was about 620.

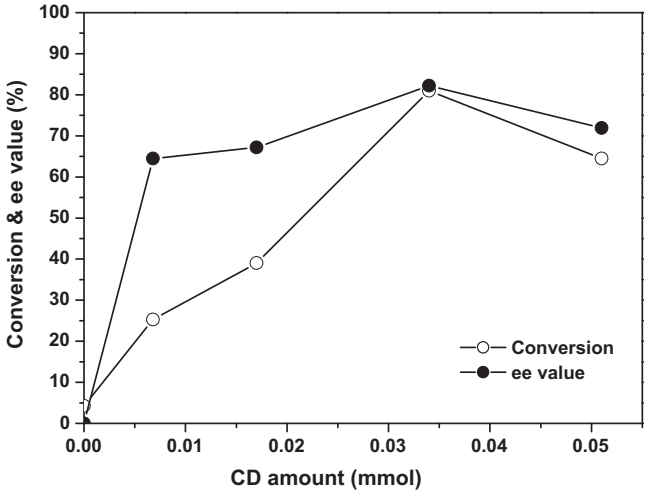

Fig. 6. Effect of CD amount on conversions and ee values in the chiral hydrogenation of ethyl pyruvate with Pt/CMK-3-W catalyst. Reaction conditions: 5 wt.% Pt/CMK-3-W catalyst (0.026 mmol Pt); ethyl pyruvate (21.07 mmol); acetic acid (20 mL); H_2 (4.0 MPa); RT; 5 min; 1200 rpm.

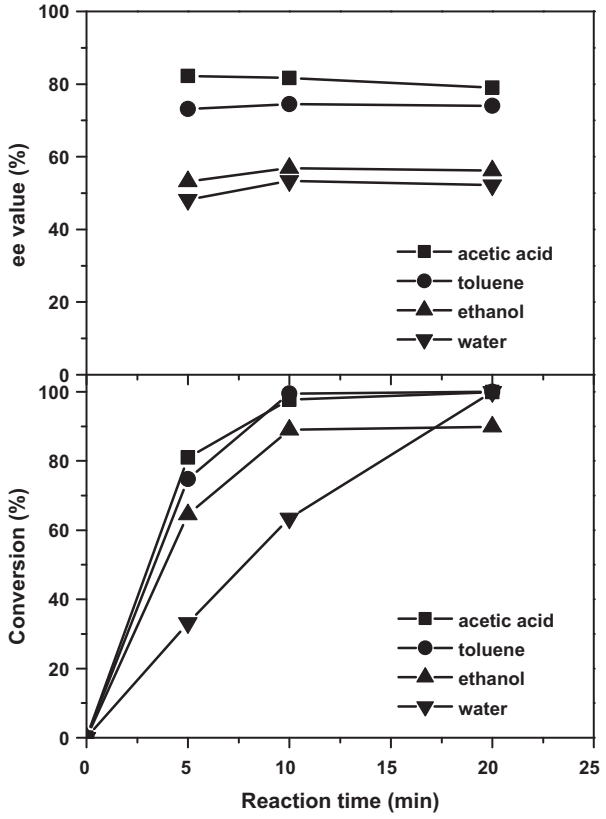

Fig. 7. Kinetic profiles of asymmetric hydrogenation of ethyl pyruvate in different solvents. Reaction conditions: 5 wt.% Pt/CMK-3-W catalyst (0.026 mmol Pt); CD (0.034 mmol); ethyl pyruvate (21.07 mmol); solvent (20 mL); H_2 (4.0 MPa); RT; 1200 rpm.

3.3. Optimization of reaction conditions for enantioselective hydrogenation of ethyl pyruvate

To optimize reaction conditions, including to screen solvent and to determine reaction time, we compared the kinetic profiles of enantioselective hydrogenation of ethyl pyruvate in acetic acid, in toluene, in ethanol and in water, respectively, with CD-modified Pt/CMK-3-W catalyst.

As shown in Fig. 7, the chiral hydrogenation of ethyl pyruvate in acetic acid ran faster than that performed in other three solvents. In acetic acid, an 81% conversion of ethyl pyruvate was obtained within 5 min and the total conversion was nearly complete within 10 min. A slightly lower ethyl pyruvate conversion of 74.8% was afforded within 5 min in toluene, and the conversion was finished within 10 min as well. Although the initial activity obtained in ethanol was not too low, furnishing a 64.5% conversion within 5 min, the reaction became sluggish and seemed stagnant after 10 min. The reaction carried out in water was the slowest, as only a 33.2% conversion was acquired within 5 min. The ee value *vs* reaction time plots in four different solvents are also displayed in Fig. 7. The enantioselectivities appeared independent on reaction time under our conditions. An 82.2% ee value was furnished in acetic acid, while 73.0%, 53.2% and 48.4% ee values were obtained in toluene, in ethanol and in water, respectively. Thus the sequence of activity and ee value obtained in different solvents was acetic acid > toluene > ethanol > water.

Solvent plays an important role in determining the reaction results for the enantioselective hydrogenation of ethyl pyruvate in a complex way, which has been discussed elsewhere [44]. The remarkable performance of chiral hydrogenation of ethyl pyruvate in acetic acid can be mainly ascribed to the protonation of quinuclidine N atom of CD, which could improve the enantioselectivity by promoting the interaction of CD with substrate through hydrogen bond [45,46]. Regarding the bad performance of the chiral hydrogenation of ethyl pyruvate in water, it can be explained by that the fine powders of quite hydrophobic CMK-3 materials are not soaked well with water, in other words, the Pt/CMK-3 catalyst is either suspended on the surface or adhered to the autoclave wall. As a result, the catalyst could not get into water to contact and adsorb substrates, hence the low activity was obtained. As for the solvent effect of toluene, it could be partly owing to the polarity of toluene. The Pt/CMK-3 catalyst could be dispersed uniformly in a single organic phase where CD and substrate are dissolved when toluene is used as solvent; therefore the substrate and chiral modifier can be easily adsorbed and/or activated by Pt/CMK-3 catalyst, resulting in high results [44]. With respect to the results obtained in ethanol, the side reaction of ethanol with ethyl pyruvate might occur in ethanol, affecting the chiral hydrogenation of ethyl pyruvate, so that the performance in ethanol was mediocre [47].

3.4. Enantioselective hydrogenation of ethyl pyruvate

Based on the findings in hand, we performed the chiral hydrogenation of ethyl pyruvate on CD-modified different Pt/CMK-3 catalysts in acetic acid and stopped the reaction after 5 min. The commercial Pt/C and Pt/Al_2O_3 catalysts were also applied for comparison.

Table 2 lists the conversions of ethyl pyruvate and ee values of (*R*)-(+)-ethyl lactate obtained on CD-modified Pt/CMK-3, Pt/C and Pt/Al_2O_3 catalysts. As above mentioned, CD-modified Pt/CMK-3-W catalyst gave 81.0% conversion together with 82.2% ee value of (*R*)-(+)-ethyl lactate (Table 2, entry 2). To investigate the calcination influence for catalyst precursors on the catalytic performance of Pt/CMK-3-W catalysts, some catalyst precursors were calcined at 423 K or at 523 K for 2 h before reduced. Compared with those obtained on Pt/CMK-3-W catalyst, the conversion of ethyl pyruvate was greatly increased to 98.3% on CD-modified Pt/CMK-3-W-423 catalyst, affording an initial activity TOF (defined as the number of moles of converted ethyl pyruvate per mole of Pt active sites per hour) higher than 23,000 h^{-1}, while the ee value was a little declined (Table 2, entries 2 *vs* 4). However, if the calcination temperature for the catalyst precursor was further elevated to 523 K, the catalytic performance of Pt/CMK-3-W-523 catalyst was sharply decreased and inferior results were afforded (Table 2, entries 2 *vs* 5).

The improvement caused by catalyst precursor calcination at a relatively lower temperature in the catalytic activity may be interpreted by that the decomposition of H_2PtCl_6 precursor and suitable Pt particle size formed during the calcination will be beneficial to the adsorption of substrate and chiral modifier; therefore, higher conversion of ethyl pyruvate was acquired on Pt/CMK-3-W-423 catalyst. As for that catalyst ever calcined at 523 K, the Pt nanoparticles were aggregated to form large particles (10.7 nm), correspondingly, lower results were obtained on Pt/CMK-3-W-523 catalyst [48].

Both the conversion (79.1%) and ee value (81.3%) obtained with Pt/CMK-3-E catalyst were a little lower than those with Pt/CMK-3-W catalyst (Table 2, entries 2 *vs* 6), although these two Pt/CMK-3 catalysts had comparable average Pt particle sizes. This probably could be interpreted by the different exposed crystal faces of Pt nanoparticles for the different Pt/CMK-3 catalysts, as both the rate and the ee increased with increasing Pt(1 1 1)/Pt(1 0 0) ratio [49].

Considering good product solubility in water, we still wonder how the Pt/CMK-3 catalyst behaves in a mixed solvent containing water, although the reaction in neat water already proved sluggish. Accordingly, we carried out the chiral hydrogenation of ethyl pyruvate with CD-modified Pt/CMK-3-W catalyst in mixed solvent containing acetic acid and water with an equal volume. To our surprise, 5 min was enough to completely convert ethyl pyruvate to the

Table 2
Reaction results obtained on chirally modified Pt/CMK-3 and related catalysts for the chiral hydrogenation of ethyl pyruvate.[a]

Entry	Catalyst	Pt size (nm)	Time (min)	Conv. (%)	ee (%)
1	CMK-3	–	5	0	0
2	Pt/CMK-3-W	2.6	5	81.0	82.2
3	Pt/CMK-3-W	2.6	5	100[b]	70.8
4	Pt/CMK-3-W-423	2.8	5	98.3	78.0
5	Pt/CMK-3-W-523	10.7	5	23.2	34.6
6	Pt/CMK-3-E	2.2	5	79.1	81.3
7	Pt/CMK-3-E	2.2	5	85.2[b]	70.5
8	Pt/C-AA	10.3	5	16.8	56.3
9	Pt/C-AA[c]	10.3	5	18.3	62.7
10	Pt/C-AA[d]	10.3	5	8.1	40.3
11	Pt/C-SA[c]	Not measured	5	18.6	60.6
12	Pt/Al_2O_3	3.5	5	98.6	92.6
13	Pt/C-AA[c]	10.3	2	9.0	65.0
14	Pt/CMK-3-W	2.6	2	24.5	71.2
15	Pt/Al_2O_3	3.5	2	19.0	87.2

[a] Reaction conditions: 5 wt.% Pt/CMK-3, Pt/C or Pt/Al_2O_3 catalyst (0.026 mmol Pt) pretreated at 673 K; CD (0.034 mmol); ethyl pyruvate (21.07 mmol); acetic acid (20 mL); H_2 (4.0 MPa); RT; 1200 rpm; and the configuration of product is *R*.
[b] The mixed solvent of acetic acid and water with a volume ratio of 1 to 1 was used.
[c] The catalyst was pretreated in a hydrogen flow at 573 K for 2 h.
[d] The catalyst was used as received.

hydrogenation product. The conversion was increased by about 20% compared with that in neat acetic acid, whereas the ee value was decreased to 70.8% as a compromise (Table 2, entry 3). Similarly, the conversion was increased from 79.1% to 85.2% while the ee value was decreased from 81.3% to 70.5% when the chiral hydrogenation of ethyl pyruvate was performed in the mixed solvent with CD-modified Pt/CMK-3-E catalyst, compared with those obtained in neat acetic acid (Table 2, entries 6 *vs* 7).

With regard to the common phenomena that the higher activity together with lower ee value on Pt/CMK-3-W and Pt/CMK-3-E catalysts is obtained in the mixed solvent of acetic acid and water, the tentative explanations may be the following two aspects. On one hand, the co-solvent water molecules maybe interact with the N atom of quinuclidine moiety in CD via hydrogen bond, so that the possibility of interaction between CD with substrate on the catalyst surface is reduced, resulting in lower ee value. On the other hand, the interaction between water and CD also decreases the competitive adsorption between CD and substrate; therefore, more Pt active sites participate in hydrogenation of substrate rather than in adsorption of CD, as a result, higher conversion of ethyl pyruvate is furnished.

The commercial 5 wt.% Pt/Al_2O_3 and Pt/C-AA catalysts were also applied to the chiral hydrogenation of ethyl pyruvate after chirally modified with CD as reference catalysts. As can be anticipated, the chirally modified Pt/Al_2O_3 catalyst showed excellent performance, obtaining 98.6% conversion together with 92.6% ee under the same conditions (Table 2, entry 12). The ee value obtained with CD-modified Pt/Al_2O_3 catalyst is higher than our home-made Pt/CMK-3 catalysts, whereas the conversion afforded with Pt/Al_2O_3 catalyst is comparable with that by Pt/CMK-3-W-423 catalyst under the same conditions. However, for the commercial Pt/C-AA catalyst, only 16.8% conversion and 56.3% ee value were afforded, much lower than those obtained with Pt/CMK-3-W catalysts (Table 2, entry 8).

In order to compete fairly between the commercial Pt/C and our home-made Pt/CMK-3 catalysts, we also studied the effect of pretreatment temperature for Pt/C-AA catalyst. As also listed in Table 2, at lower pretreatment temperature such as 573 K in a hydrogen flow looks like more reasonable for Pt/C-AA catalyst, as slightly higher conversion (18.3%) and ee value (62.7%) were achieved (entry 9); while the Pt/C-AA catalyst used as received gave the lowest results (Table 2, entry 10). Although the optimization of pretreatment method for Pt/C-AA catalyst could somewhat improve the catalytic performance, the results were much lower than those obtained with our home-made Pt/CMK-3-W catalyst. Moreover, the other commercial 5 wt.% Pt/C-SA catalyst purchased from Sigma–Aldrich was also applied as a reference. This commercial Pt/C-SA catalyst furnished quite similar results to the other one (Table 2, entry 11).

In addition, we also carried out the asymmetric hydrogenation of ethyl pyruvate within 2 min in order to better evaluate and compare the catalytic activity between different catalysts. As still listed in Table 2 (entries 13–15), the initial activity with Pt/CMK-3-W catalyst was the highest among the three Pt catalysts. It seemed that there had an induction period for the Pt/CMK-3-W and the Pt/Al_2O_3 catalysts. We deduce that the good performance of Pt/CMK-3 catalyst, compared with commercial Pt/C catalysts, can be partly attributed to the periodic mesoporous structure features of CMK-3 OMCs that are advantageous to mass transport as the CMK-3 OMCs indeed have the larger specific surface area and larger pore volume. The smaller Pt particle size of Pt/CMK-3-W catalyst is beneficial to higher conversion compared with Pt/C catalysts as well.

Besides the catalytic performance, the stability of Pt/CMK-3 catalyst is also an important matter to consider. Hence we detected the leached Pt atoms in the filtrate after the chiral hydrogenation in acetic acid by the ICP-AES firstly. To our delight, only below 0.005% Pt atoms were leached for the Pt/CMK-3-W catalyst under our conditions, while for the commercial Pt/Al_2O_3 and Pt/C-AA catalyst, the leached amount was up to 0.15% and 0.25%, respectively. Furthermore, the reusability of CD-chirally modified Pt/CMK-3-W, Pt/C-AA and Pt/Al_2O_3 catalysts in the asymmetric hydrogenation of ethyl pyruvate was also investigated and compared. Just as shown in Fig. 8, the Pt/CMK-3-W catalyst can be reused for more than 5 times without distinct loss of activity and enantioselectivity. However, for the commercial Pt/C-AA and Pt/Al_2O_3 catalysts, the reusability was poor, and the conversion was markedly decreased with reaction runs. The mediocre reusability of Pt/Al_2O_3 catalyst could be mainly owing to the Pt leaching and to the peptization of alumina support in acidic medium. The good stability of Pt/CMK-3 catalyst might be ascribed to that the Pt nanoparticles can be stabilized through the π-donating interaction from the disordered graphene of CMK-3 OMCs [42].

3.5. Enantioselective hydrogenation of EOPB

In order to broaden the substrate scope, we also applied the Pt/CMK-3 catalysts to the chiral hydrogenation of EOPB. It has been discovered that (*R*)-(+)-ethyl-2-hydroxy-4-phenylbutyrate,

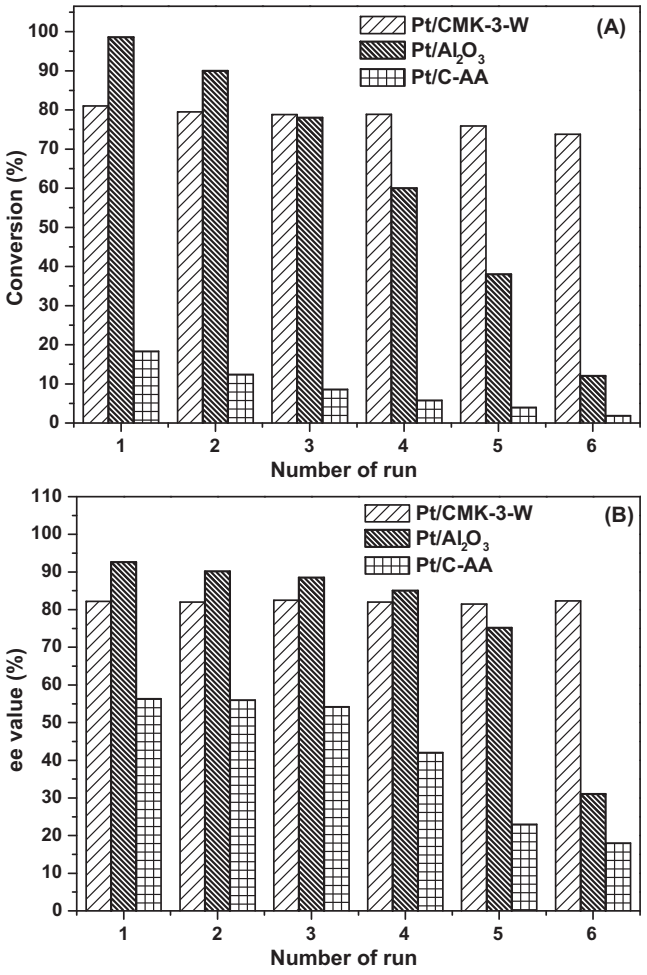

Fig. 8. Reusability of Pt/CMK-3-W, Pt/C-AA and Pt/Al_2O_3 catalysts in the asymmetric hydrogenation of ethyl pyruvate in acetic acid. Reaction conditions: Pt catalyst (0.026 mmol Pt); CD (0.034 mmol); ethyl pyruvate (21.07 mmol); acetic acid (20 mL); H_2 (4.0 MPa); RT; 5 min; 1200 rpm.

the hydrogenation product of asymmetric hydrogenation of EOPB, can be widely used in the preparation of chiral medicine Enalapril, which then can be used in therapy of many important symptoms such as hypertension and myocardial infarction [50].

As acetic acid has been proved to be better solvent whereas Pt/CMK-3-W-523 catalyst showed bad performance in the chiral hydrogenation of ethyl pyruvate, we only applied Pt/CMK-3-W, Pt/CMK-3-E and Pt/CMK-3-W-423 catalysts to the chiral hydrogenation of EOPB in acetic acid. As listed in Table 3, higher than 93% conversions were obtained within 5 min on CD-modified Pt/CMK-3 catalysts in acetic acid (Table 3, entries 1–3). The highest TOF of higher than 5600 h^{-1} with 64.3% ee value was obtained on CD-modified Pt/CMK-3-W-423 catalyst (Table 3, entry 3). The ee values obtained on Pt/CMK-3-W and Pt/CMK-3-W-423 catalyst were comparable under the same conditions, whereas a comparatively lower ee value was achieved on Pt/CMK-3-E catalyst (Table 3, entry 2).

Table 3
Reaction results obtained on chirally modified Pt/CMK-3 and related catalysts for the chiral hydrogenation of EOPB.[a]

Entry	Catalyst	Pt size (nm)	Conv. (%)	ee (%)
1	Pt/CMK-3-W	2.6	93.7	63.4
2	Pt/CMK-3-E	2.2	93.9	50.3
3	Pt/CMK-3-W-423	2.8	93.4	64.3
4	Pt/C-AA	10.3	70.0	64.8
5	Pt/C-AA[b]	10.3	72.0	65.7
6	Pt/Al_2O_3	3.5	98.6	83.5

[a] Reaction conditions: 5 wt.% Pt/CMK-3, Pt/C or Pt/Al_2O_3 catalyst (0.026 mmol Pt) pretreated at 673 K; CD (0.034 mmol); EOPB (5.29 mmol); acetic acid (20 mL); H_2 (4.0 MPa); RT; 1200 rpm; 5 min, and the configuration of product is *R*.
[b] The catalyst was pretreated in a hydrogen flow at 573 K for 2 h.

Of particular note is that the difference between the catalytic activities obtained with different Pt/CMK-3 catalysts for the chiral hydrogenation of EOPB can be negligible, while the difference between the ee values achieved with Pt/CMK-3-W and Pt/CMK-3-E catalysts was enlarged. The trend in the chiral hydrogenation of EOPB is little different from that in the chiral hydrogenation of ethyl pyruvate. This perhaps could be interpreted partly by the molecular size of EOPB, which bears a benzene ring with comparatively large size. The Pt/CMK-3-E catalyst has the smallest Pt particle size of about 2.2 nm, which may be not beneficial to the co-adsorption of CD and EOPB on its surface simultaneously, so that some EOPB molecules were hydrogenated without participation of chiral modifier and accordingly, a little inferior ee value was afforded. In addition, it is that the diffusion of reactants and products probably plays an important role in determining the catalytic activity in the chiral hydrogenation of EOPB, therefore, the differences such as metal–support interaction and catalyst surface affinity become less important. This phenomenon is very similar to that previously observed for Pt/Al_2O_3 catalyst in the same reaction [51].

The reference catalyst 5 wt.% Pt/Al_2O_3 also worked well in the asymmetric hydrogenation of EOPB by modification with CD and better results were obtained (Table 3, entry 6). The 5 wt.% Pt/C-AA catalyst gave lower conversions of EOPB than the Pt/CMK-3 catalyst did, but the ee values afforded with the two catalysts were comparable (Table 3, entries 1 *vs* 4 and 5).

3.6. IR spectroscopic characterization of Pt/CMK-3 catalyst

The surface property of support material would inevitably affect adsorption and dispersion of Pt nanoparticles on the support. As already characterized by Raman spectroscopy, the CMK-3 carbons mainly consist of the disordered graphene, which have plenty of π electrons on the surface. Compared with CMK-3, the unsaturated coordinated Al^{3+} species make the Al_2O_3 surface electron-deficient [52]. In order to identify how the surface property of Pt catalyst affect the catalytic performance, the Pt/CMK-3-W and Pt/Al_2O_3 catalysts were further characterized by IR spectroscopy using CO as probe molecules.

Fig. 9 shows the DRIFT spectra of CO adsorbed on Pt/CMK-3-W and on Pt/Al_2O_3 catalysts at 308 K. For CO linearly adsorbed on commercial Pt/Al_2O_3 catalysts, a band at 2083 cm^{-1} together with a weak shoulder peak at 2050 cm^{-1} was observed (Fig. 9c). The IR band at 2083 cm^{-1} can be attributed to CO linearly adsorbed on Pt atoms with somewhat positive charge $Pt^{\delta+}$ sites derived from the strong interaction of Pt with Al_2O_3, while the broad IR band centered at 2050 cm^{-1} can be assigned to CO adsorbed on Pt^0 atoms. Regarding CO adsorbed on Pt/CMK-3, the linearly adsorbed CO almost disappeared after the sample was purged with helium (Fig. 9d), although an extremely weak band at about 2060 cm^{-1} was observed when CO adsorption was saturated (Fig. 9b). It is suggested that the adsorption of CO on the Pt/CMK-3 surface is very weak, due to the electrostatic repulsion between CO molecules and π electrons from the disordered graphene on the CMK-3 surface with a high electron density.

Compared with the commercial Pt/Al_2O_3 catalyst surface, the Pt/CMK-3 catalyst surface with a high electron density would increase feedback bonding from d orbital of Pt atoms to $2\pi^*$ orbital of C=O double bond in ethyl pyruvate, so that the C=O bond energy was decreased and accordingly the C=O double band can be easily broken. As a result, the substrate can be easily activated by Pt^0 atoms of Pt/CMK-3 catalyst, although the adsorption of reactant

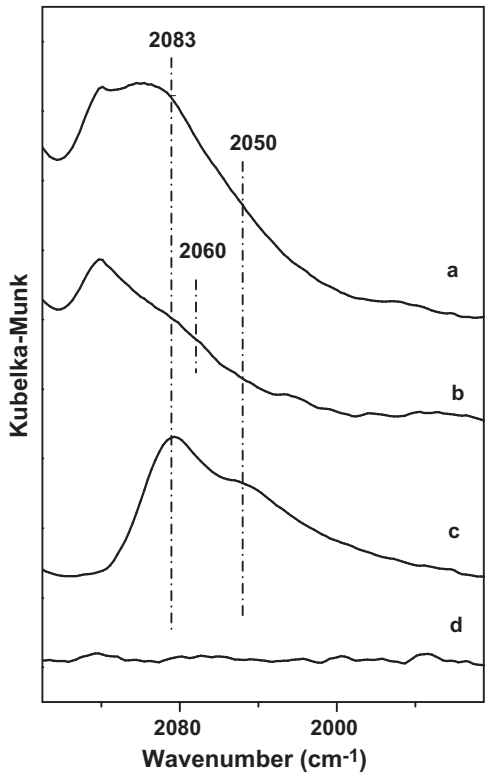

Fig. 9. DRIFT spectra of CO adsorbed on (a) Pt/Al_2O_3 catalyst, CO saturated; (b) Pt/CMK-3-W catalyst, CO saturated; (c) Pt/Al_2O_3 catalyst, He purged; (d) Pt/CMK-3-W catalyst, He purged.

may be weakened due to the repulsive interaction of Pt/CMK-3 surface with a high electron density. Furthermore, Pt/CMK-3 catalysts with ordered mesoporous structure also had high specific surface area, adequate pore volume and small Pt particle size with high dispersion, which enables easy mass transport, hence comparable conversion in the chiral hydrogenation of ethyl pyruvate can be achieved on CD-modified Pt/CMK-3 catalysts. Additionally, the weak interaction of CO with Pt/CMK-3 catalyst can also deduce that CD was also weakly adsorbed on the catalyst surface because the high electron density from the disordered graphene of Pt/CMK-3 surface maybe hinders the adsorption of quinoline moiety of CD through the π interaction. Therefore, lower ee values were furnished by CD-modified Pt/CMK-3 catalysts. Nevertheless, the high electron density of CMK-3 support can also result in the strong π donating interaction to stabilize the Pt nanoparticles, as a result, only trace amount of Pt atoms were leached into the solution and the Pt/CMK-3-W catalyst showed good reusability.

4. Conclusion

5 wt.% Pt/CMK-3 catalysts were prepared via a facile impregnation method using H_2PtCl_6 dissolved in different media as Pt precursors. After chirally modified with cinchona alkaloids, Pt/CMK-3 catalysts proved to be active and enantioselective for the enantioselective hydrogenation of α-ketoesters under mild conditions. The initial activity of higher than 23,000 h^{-1} TOF and up to 82% ee were obtained with CD-modified Pt/CMK-3 catalysts for the chiral hydrogenation of ethyl pyruvate. With regard to the asymmetric hydrogenation of ethyl 2-oxo-4-phenylbutyrate, the highest TOF of 5615 h^{-1} and 64% ee were afforded. To the best of our knowledge, the results achieved in this study with Pt/CMK-3 catalyst are the best ones among those obtained with Pt catalysts supported on carbon materials, including activated carbon, carbon nanotubes and ordered mesoporous carbons. Of particular note is that the stability of Pt/CMK-3 catalyst was higher than the commercial Pt/Al_2O_3 and Pt/C catalysts and Pt/CMK-3 catalyst also afforded comparable ethyl pyruvate conversion with Pt/Al_2O_3 catalyst.

Acknowledgements

This work was supported by the NSFC (20703018) and Shanghai Leading Academic Discipline Project (B409). The authors thank Mr. Zhen Liu for his help in Raman spectrum measurements.

References

[1] T. Burgi, A. Baiker, Acc. Chem. Res. 37 (2004) 909.
[2] M. Studer, H.U. Blaser, C. Exner, Adv. Synth. Catal. 345 (2003) 45.
[3] M. Bartok, Curr. Org. Chem. 10 (2006) 1533.
[4] M. Studer, S. Burkhardt, H.U. Blaser, Chem. Commun. (1999) 1727.
[5] A. Baiker, Catal. Today 100 (2005) 159.
[6] D.Y. Murzin, P. Maki-Arvela, E. Toukoniitty, T. Salmi, Catal. Rev.: Sci. Eng. 47 (2005) 175.
[7] G.J. Hutchings, Annu. Rev. Mater. Res. 35 (2005) 143.
[8] T. Mallat, E. Orglmeister, A. Baiker, Chem. Rev. 107 (2007) 4863.
[9] Y. Orito, S. Imai, S. Niwa, Preprints of the 43rd Catalysis Forum (Japan, 1978), 1978, p. 130.
[10] Y. Orito, S. Imai, S. Niwa, J. Chem. Soc. Jpn. 8 (1979) 1118.
[11] Y. Orito, S. Imai, S. Niwa, J. Chem. Soc. Jpn. 1 (1982) 137.
[12] B. Torok, K. Felfoldi, G. Szakonyi, K. Balazsik, M. Bartok, Catal. Lett. 52 (1998) 81.
[13] B. Torok, K. Balazsik, M. Torok, Gy. Szollosi, M. Bartok, Ultrason. Sonochem. 7 (2000) 151.
[14] M. Bartok, K. Balazsik, G. Szollosi, T. Bartok, J. Catal. 205 (2002) 168.
[15] S.P. Griffiths, P. Johnston, P.B. Wells, Appl. Catal. A: Gen. 191 (2000) 193.
[16] B. Torok, G. Szollosi, K. Balazsik, K. Felfoldi, I. Kun, M. Bartok, Ultrason. Sonochem. 6 (1999) 97.
[17] M.Y. Kim, S.B. Jung, M.G. Kim, Y.S. You, J.H. Park, C.H. Shin, G. Seo, Catal. Lett. 129 (2009) 194.
[18] S. Basu, M. Mapa, C.S. Gopinath, M. Doble, S. Bhaduri, G.K. Lahiri, J. Catal. 239 (2006) 154.
[19] U. Bohmer, F. Franke, K. Morgenschweis, T. Beiber, W. Reschitilowski, Catal. Today 60 (2000) 167.
[20] X. Li, Y. Shen, R. Xing, Y. Liu, H. Wu, M. He, P. Wu, Catal. Lett. 122 (2008) 325.
[21] X. Li, Ph.D Thesis, School of Graduate Students, Chinese Academy of Sciences, (2004).
[22] Y. Orito, S. Imai, S. Niwa, G.H. Nguyen, J. Synth. Org. Chem. Jpn. 37 (1979) 173.
[23] M. Fraga, M. Mendes, E. Jordao, J. Mol. Catal. A: Chem. 179 (2002) 243.
[24] A. Perosa, P. Tundo, M. Selva, J. Mol. Catal. A: Chem. 180 (2002) 169.
[25] J.T. Wehrli, A. Baiker, D.M. Monti, H.U. Blaser, H.P. Jalett, J. Mol. Catal. 57 (1989) 245.
[26] L. Xing, F. Du, J. Liang, Y. Chen, Q. Zhou, J. Mol. Catal. A: Chem. 276 (2007) 191.
[27] G. Szollosi, Z. Nemeth, K. Hernadi, M. Bartok, Catal. Lett. 132 (2009) 370.
[28] G. Farkas, L. Hegedus, A. Tungler, T. Mathe, J. Figueiredo, M. Freitas, J. Mol. Catal. A: Chem. 153 (2000) 215.
[29] E. Sipos, G. Fogassy, A. Tungler, P. Samant, J. Figueiredo, J. Mol. Catal. A: Chem. 212 (2004) 245.
[30] T. Tarnai, A. Tungler, T. Mathe, J. Petro, R.A. Sheldon, G. Toth, J. Mol. Catal. A: Chem. 102 (1995) 41.
[31] E. Sipos, A. Tungler, I. Bitter, React. Kinet. Catal. Lett. 79 (2003) 101.
[32] R. Ryoo, S.H. Joo, M. Kruk, M. Jaroniec, Adv. Mater. 13 (2001) 677.
[33] R. Ryoo, S.H. Joo, Stud. Surf. Sci. Catal. 148 (2004) 241.
[34] J. Lee, S. Han, T. Hyeon, J. Mater. Chem. 14 (2004) 478.
[35] T. Ohkubo, J. Miyawaki, K. Kaneko, R. Ryoo, N.A. Seaton, J. Phys. Chem. B 106 (2002) 6523.
[36] L. Li, Z.H. Zhu, G.Q. Lu, Z.F. Yan, S.Z. Qiao, Carbon 45 (2007) 11.
[37] D. Su, J. Delgado, X. Liu, D. Wang, R. Schlogl, L. Wang, Z. Zhang, Z. Shan, F. Xiao, Chem. Asian J. 4 (2009) 1108.
[38] J. Lee, S. Yoon, T. Hyeon, S.M. Oh, K.B. Kim, Chem. Commun. (1999) 2177.
[39] M. Kang, S.H. Yi, H.I. Lee, J.E. Yie, J.M. Kim, Chem. Commun. (2002) 1944.
[40] M. Choi, R. Ryoo, Nat. Mater. 2 (2003) 473.
[41] S. Jun, S. Joo, R. Ryoo, M. Kruk, J. Am. Chem. Soc. 122 (2000) 10712.
[42] R. Xing, Y. Liu, Y. Wang, L. Chen, H. Wu, Y. Jiang, M. He, P. Wu, Micropor. Mesopor. Mater. 105 (2007) 41.
[43] M.S. Dresselhaus, A. Jorio, M. Hofmann, G. Dresselhaus, R. Saito, Nano Lett. 10 (2010) 751.
[44] Z. Ma, F. Zaera, J. Phys. Chem. B 109 (2005) 406.
[45] M. Arx, T. Burgi, T. Mallat, A. Baiker, Chem. Eur. J. 8 (2002) 1430.
[46] M. Minder, T. Mallat, P. Skrabal, A. Baiker, Catal. Lett. 29 (1994) 115.
[47] D. Ferri, T. Burgi, K. Borszeky, T. Mallat, J. Catal. 193 (2000) 139.
[48] D. Radivojevic, K. Seshan, L. Lefferts, Appl. Catal. A: Gen. 301 (2006) 51.
[49] E. Schmidt, A. Vargas, T. Mallat, A. Baiker, J. Am. Chem. Soc. 131 (2009) 12358.
[50] M.R. Attwood, C.H. Hassall, A. Krohn, G. Lawton, S. Redshaw, J. Chem. Soc. Perkin Trans. I (1986) 1011.
[51] X. Li, X. You, P. Ying, J. Xiao, C. Li, Top. Catal. 25 (2003) 63.
[52] V.M. Bermudez, J. Phys. Chem. C 113 (2009) 1917.